ISSN: 2688-8645

Design and Optimization of a Layered Polymer Injection Flow Control Valve for Enhanced Oil Recovery via Polymer Flooding

Haifeng Ma *, Taiyu Chen, Xinxin Yan

School of Mechatronic Engineering, SouthWest Petroleum University, Chengdu, Sichuan, 610500, China

* Corresponding author: Haifeng Ma

Abstract

Focusing on the issue of severe viscosity loss in the flow control valve, a core component of polymer flooding for enhanced oil recovery, this study takes the layered polymer injection flow control valve as the research object. A numerical simulation and structural optimization based on low shear rate conditions were conducted, and experiments were performed to verify the feasibility of the optimized design. Using the control variable method, numerical simulations were carried out on different valve spool structures, slot spacing, slot depth, and valve stem length. The results demonstrate that the circular arc spool flow control valve exhibits superior viscosity preservation performance compared to other shapes. When the slot spacing is 30 mm, slot depth is 3 mm, and valve stem length is 1 mm, the viscosity preservation performance is optimal. Orthogonal experiments reveal that slot depth has the most significant impact on shear rate and validate the accuracy of single-factor analysis. Field experiments measured a maximum viscosity loss rate of 8.9%, which is a significant improvement compared to the 12% loss observed in other oilfields, confirming the enhanced viscosity preservation effect of the optimized flow control valve. This study provides theoretical support for the optimization of layered polymer injection tools.

Keywords

Flow Control Valve; Arc-Shaped Spool; Numerical Simulation; Shear Rate; Viscosity Loss Rate.

1. Introduction

With the continuous advancement of petroleum extraction technologies, Tertiary Recovery (Enhanced Oil Recovery, EOR) methods—incorporating physical, chemical, and biological approaches—have been progressively implemented. Currently, major domestic oilfields have transitioned into the middle and late stages of development. The conventional waterflooding methods used in secondary recovery have resulted in water cuts exceeding 90%, rendering the efficient extraction of residual oil from reservoirs increasingly difficult[1]. In recent years, EOR technologies have primarily focused on thermal recovery, gas injection, and chemical flooding. Among these, polymer flooding has been widely adopted across major domestic oilfields due to its suitability for China's continental heterogeneous reservoirs and its lower environmental impact compared to other chemical agents. The principle of polymer flooding involves injecting water-soluble high-molecular-weight polymers into the water to increase its viscosity and reduce the oil-water mobility ratio, thereby enhancing crude oil mobility and facilitating its displacement from subsurface reservoirs[2]. These displacement polymers are non-Newtonian fluids; their macromolecular long-chain structures provide high viscoelasticity, which can stretch oil droplets and films to enhance carrying capacity. However, these polymer chains are

ISSN: 2688-8645

susceptible to mechanical degradation under high shear stress, leading to significant viscosity loss.

During the injection process, viscosity loss primarily occurs as the polymer passes through flow control valves at high velocities[3-7]. Consequently, the design of polymer injection tools must prioritize low-shear-rate flow fields to minimize viscosity degradation. Several researchers, both domestically and internationally, have conducted studies on the low-shear design of tool flow fields. For instance, Meng et al.[8] developed a shuttle-shaped rod annular flow channel structure that significantly reduces viscosity loss in zonal injection mandrels. Paiva et al.[9] evaluated an intermittent flow pattern regulator and found it effective in maintaining viscosity. Sun et al.[10] identified the fundamental causes of viscosity loss and proposed a streamlined multi-stage valve core structure. Ren et al.[11] discovered that maintaining a flow trajectory approximating laminar flow can minimize frictional losses. Han et al.[12] designed a novel injection tool with superior technical performance. Zhang et al.[13] found that under identical water-cut conditions, the equivalent shear rate increases with the gas-liquid ratio. Husveg et al.[14] developed a new low-shear valve based on cyclone technology with positive results. Zhang et al.[15] completed the general design of a wireline-retrievable intelligent water injector featuring a valve-core structure.

In summary, there is currently limited research specifically targeting polymer injection flow control valves, despite them being core components of the injection process. To address this, this paper proposes a model for a zonal polymer injection flow control valve and conducts a simulation-based study, the results of which are applied to field experiments. Zonal injection technology enables real-time monitoring and regulation of parameters such as injection volume, pressure, and temperature for each layer. This not only provides a theoretical foundation for the optimization of zonal injection tools but also opens new research avenues for the intelligent development of deep-well polymer injection processes.

2. Zonal Polymer Injection Flow Control Valve

The polymer injection mandrel (working barrel) serves as the core equipment in zonal polymer injection technology. Its critical component, the flow control valve, regulates the injection rate for each reservoir layer by adjusting the valve opening, which directly determines the efficiency of polymer flooding. Figure 1 illustrates the 3D structural diagram of the flow regulation mechanism. This mechanism primarily consists of a motor, a lead screw mechanism (screw mechanism), limit switches, a drive shaft, sealing devices, the flow control valve core (plug), and the valve sleeve (seat).

When the motor is activated, it drives the lead screw mechanism, which converts the rotational motion of the motor into axial displacement. This motion translates the drive shaft and the valve core assembly axially, thereby achieving the precise adjustment of the valve opening.

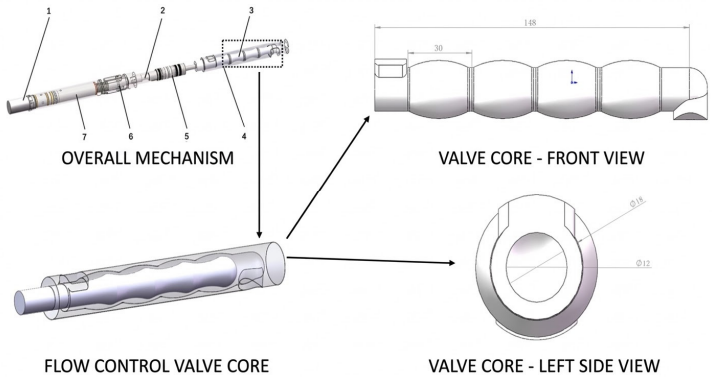

Fig 1. Three-dimensional Structural Diagram of Flow Control Mechanism

ISSN: 2688-8645

The components are identified as follows: 1-Motor; 2-Drive shaft; 3-Flow control valve core (plug); 4-Flow control valve sleeve; 5-Sealing device; 6-Limit switch; and 7-Lead screw mechanism. Upon activation, the motor drives the lead screw mechanism, which converts rotational motion into axial displacement. This motion translates the drive shaft and the valve core assembly simultaneously, thereby achieving the desired adjustment of the valve opening.

The focus of this study is the internal flow field of the flow control valve, which features a single-inlet and single-outlet configuration. Table 1 summarizes the boundary condition settings for the numerical simulation. The inlet is defined as a velocity inlet (with a flow velocity of 5.05 m/s), and the outlet is set as a pressure outlet (with a static pressure of 0 Pa). All other wall surfaces are assigned adiabatic, no-slip boundary conditions.

Table 1. Numerical Simulation Boundary Condition Setup for Flow Control Valve

Wall Boundary	Inlet Boundary	Outlet Boundary	Fluid Medium
Adiabatic and No-slip Conditions	Velocity-inlet	Pressure-outlet	APP4

By varying the global and local mesh sizes of the external flow field surrounding the valve core, multiple computational models with different mesh densities were generated. Identical boundary conditions and operational parameters were applied to monitor the **average shear rate** across the valve core and the **pressure differential** between the inlet and outlet. The results are illustrated in Figure 2. It is evident that when the mesh count reaches **2.8 million**, the influence of mesh density on the computational results becomes negligible. Therefore, considering both computational accuracy and efficiency, a mesh count of 2.8 million was selected as the standard for subsequent simulations.

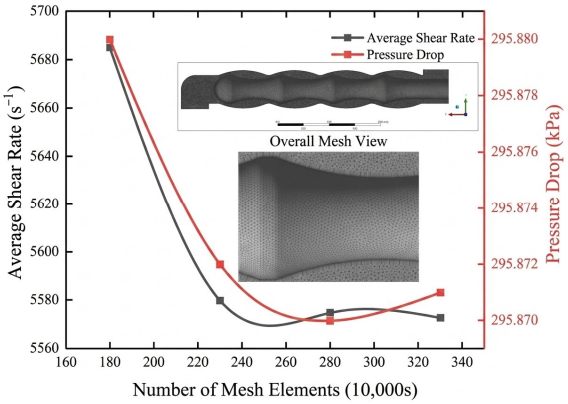

Fig 2. Mesh Generation and Mesh Independence Verification

3. Simulation Analysis of Polymer Viscosity Loss

To identify the optimal flow channel configuration, this paper designs four valve core structures with similar diameters and lengths: triangular, shuttle-shaped, trapezoidal, and arc-shaped, as illustrated in Figure 3. A numerical simulation based on low-shear-rate criteria was conducted on the flow control valve during the polymer injection process. This study aims to optimize the valve body configuration and its structural parameters to minimize viscosity loss and enhance oil displacement efficiency. The viscosity retention performance of the valve body is analyzed and discussed from the perspectives of different valve core geometries and their respective structural parameters.

ISSN: 2688-8645

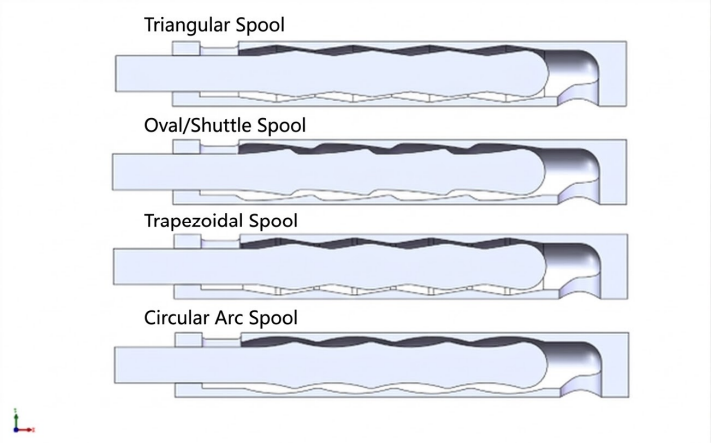

Fig 3. Four types of structural models of valve spool

3.1. Influence of Different Valve Core Structures on Shear Rate

Numerical simulations were performed for the four aforementioned valve core structures at various openings under a constant flow rate to evaluate their respective viscosity retention performances.

Figure 4 presents a comparison of the shear rates for the different valve cores at openings ranging from 25% to 100%. It is observed from the results that both the average shear rate and the maximum shear rate of the arc-shaped valve core remain the lowest across all openings. Its viscosity retention capability is approximately 3% higher than that of the shuttle-shaped valve core, which ranks second. These findings demonstrate that among the four candidate geometries, the arc-shaped valve core provides the superior viscosity retention effect.

The results indicate that, under identical conditions, the flow channels of the arc-shaped valve core and the circular valve head exhibit superior viscosity retention performance compared to the other configurations. Consequently, subsequent numerical simulations will focus on the arc-shaped valve core to analyze the effects of varying groove spacing, groove depth, and segment length. This analysis aims to identify the optimal structural parameters for maximizing the viscosity retention effect.

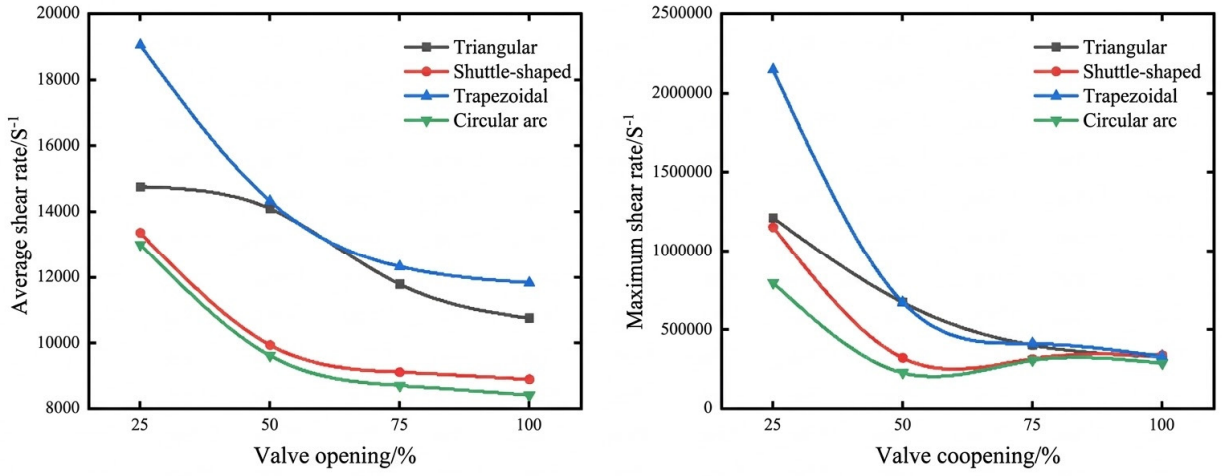

(a) Average shear rate for different shear rapes (b) Maximum shear rate for Maximum shear rates

Fig 4. Shear Rate Curves for Four Spool Shapes at Different Openings

3.2. Influence of Arc-Shaped Valve Core Geometric Parameters on Shear Rate

To further investigate the impact of the arc-shaped valve core on polymer viscosity loss, this section adopts the control variable method to analyze the influence of individual structural parameters on the shear rate. Given that the flow channels formed by the inner wall of the valve

ISSN: 2688-8645

body and the outer wall of the valve core consist of periodically repeating geometries, the analysis of viscosity retention performance focuses on the structural parameters of a single valve stage. The primary geometric parameters of a single-stage valve core include the groove spacing (L), the groove depth (H), and the segment length (W).

3.2.1. Analysis of the Influence of Valve Core Groove Spacing on Shear Rate

Based on the arc-shaped valve core structure, numerical simulations were conducted to analyze the flow characteristics of the internal field across different groove spacings, while maintaining a constant groove depth and segment length. The groove spacing (L) was varied from 26 mm to 30 mm, with an incremental step of 0.1 mm.

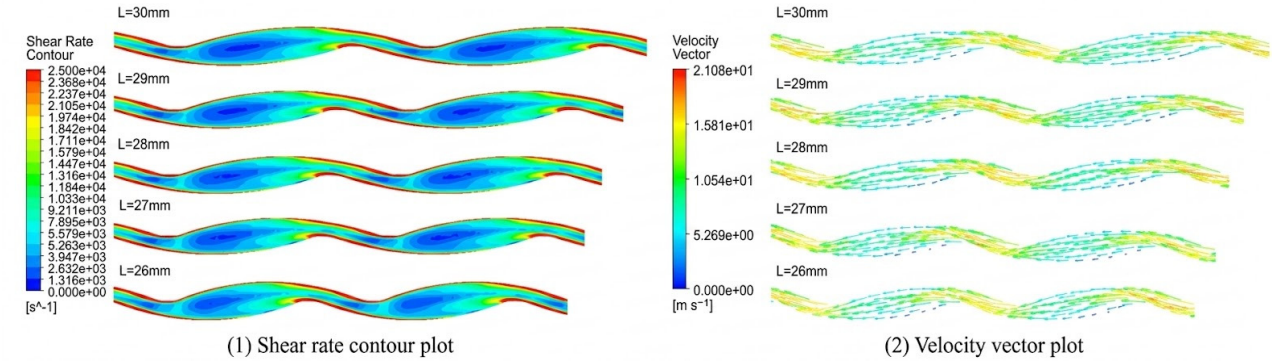

Fig 5. Analysis Contour Plot for Different Slot Spacing

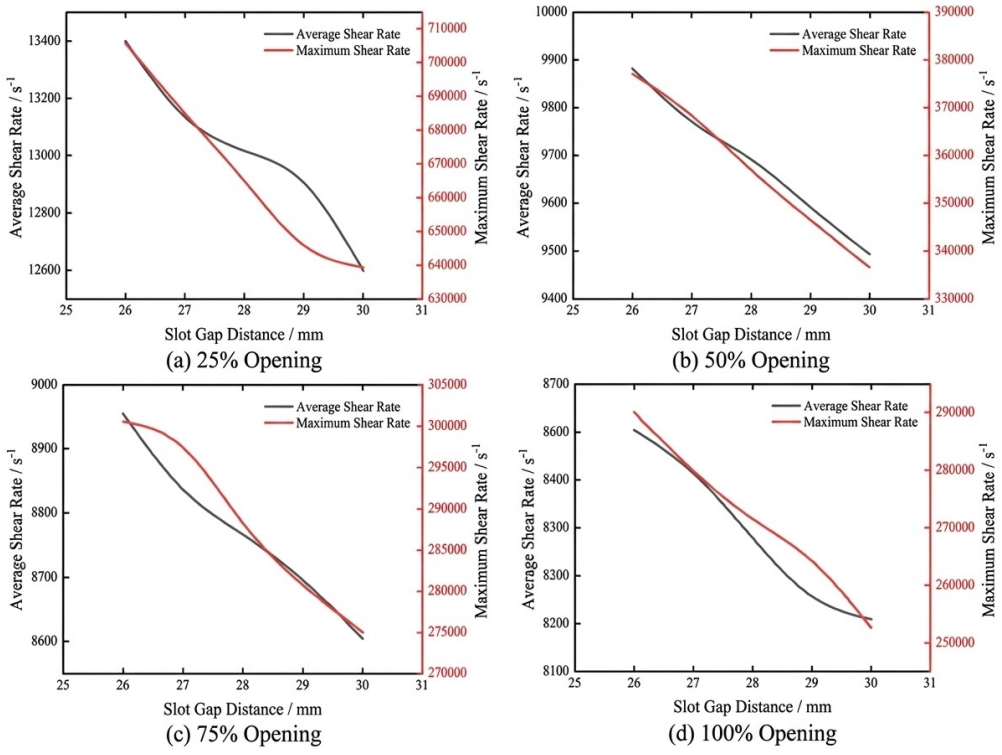

Fig 6. Analysis Result Curve Chart for Different Slot Spacing

Figure 5 presents the shear rate contours (1) and velocity vector plots (2) for various groove spacings under an inlet flow rate of 5 m^3/h and a valve opening of 50%. The results indicate that peak shear rates predominantly occur at the wall surfaces where the flow channel geometry undergoes abrupt changes. Specifically, an increase in the shear rate is observed at every contraction point within the flow path, with the maximum shear rate localized at the tangency point between the channel outlet and the wall surface. At the narrowest sections of

ISSN: 2688-8645

the flow channel, the fluid velocity undergoes sudden variations, resulting in steep velocity gradients and, consequently, elevated shear rates. As the groove spacing increases, the velocity transitions become more gradual, leading to reduced velocity gradients and lower shear rates.

Figure 6 illustrates the comparison of the average and maximum shear rates across valve openings ranging from 25% to 100%. The curves clearly demonstrate a strong negative correlation between the groove spacing and both shear rate metrics across all four opening scenarios. As the groove spacing increases, both the average and maximum shear rates exhibit a consistent decline.

The results show that increasing the groove spacing from 26 mm to 30 mm effectively reduces the shear rate. The arc-shaped valve core with a 30 mm groove spacing achieves the lowest shear rate and superior viscosity retention performance. Therefore, 30 mm is identified as the optimal groove spacing.

3.2.2. Analysis of the Influence of Valve Core Groove Depth on Shear Rate

Furthermore, while maintaining a consistent segment length and a fixed groove spacing of 30 mm, numerical simulations were performed to analyze the flow characteristics of the internal field across various groove depths (H). The groove depth was varied from 1.5 mm to 3.5 mm, with an incremental step of 0.1 mm.

Figure 7 presents the shear rate distribution contours (1) and velocity vector plots (2) for different groove depths under an inlet flow rate of 5 m^3/h, a valve opening of 50%, and a groove spacing of 30 mm. The results indicate that the shear rates at the flow channel walls are consistently higher than those at the center, with the shear rate decreasing as the distance from the center increases. This phenomenon is primarily attributed to the fact that the shear rate is predominantly governed by the velocity gradient; the velocity gradient is steepest near the channel walls and diminishes toward the center. Additionally, it is observed that the shear rate within the flow channel decreases as the groove depth increases. At a groove depth of 1.5 mm, the shear rate in the narrower sections of the channel is significantly higher than that at other depths. This is because an increase in groove depth leads to a reduction in the average flow velocity within the channel, thereby lowering the internal velocity gradient and the resulting shear rate.

Figure 8 illustrates the comparison of the average and maximum shear rates for different groove depths across valve openings ranging from 25% to 100%. The curves clearly demonstrate a general negative correlation between groove depth and shear rate across all four opening scenarios. Although the shear rate generally decreases as the groove depth increases, both the average and maximum shear rates exhibit an upward trend at a groove depth of 3.5 mm. This increase is caused by the emergence of vortex phenomena (vortices) within the flow channel at this specific depth.

The results indicate that the groove depth (1.5–3.5 mm) is generally negatively correlated with the shear rate. The arc-shaped valve core with a 3 mm groove depth achieves the lowest shear rate and demonstrates superior viscosity retention performance. Consequently, 3 mm is identified as the optimal groove depth.

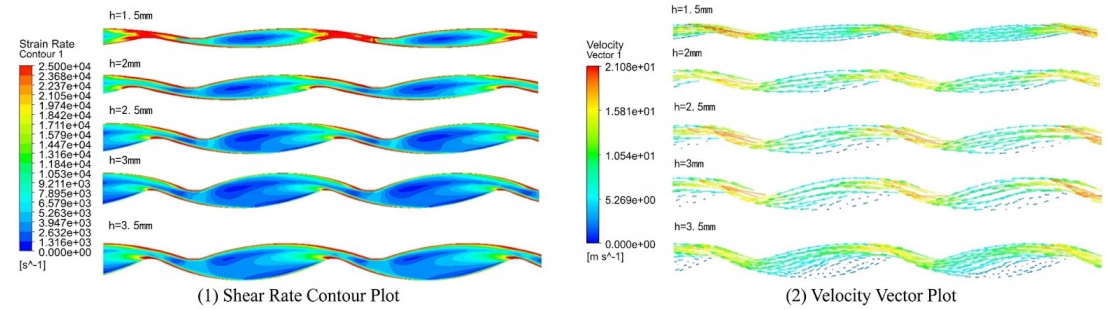

(1) Shear Rate Contour Plot (2) Velocity Vector Plot

Fig 7. Analysis Contour Plot for Different Slot Depths

ISSN: 2688-8645

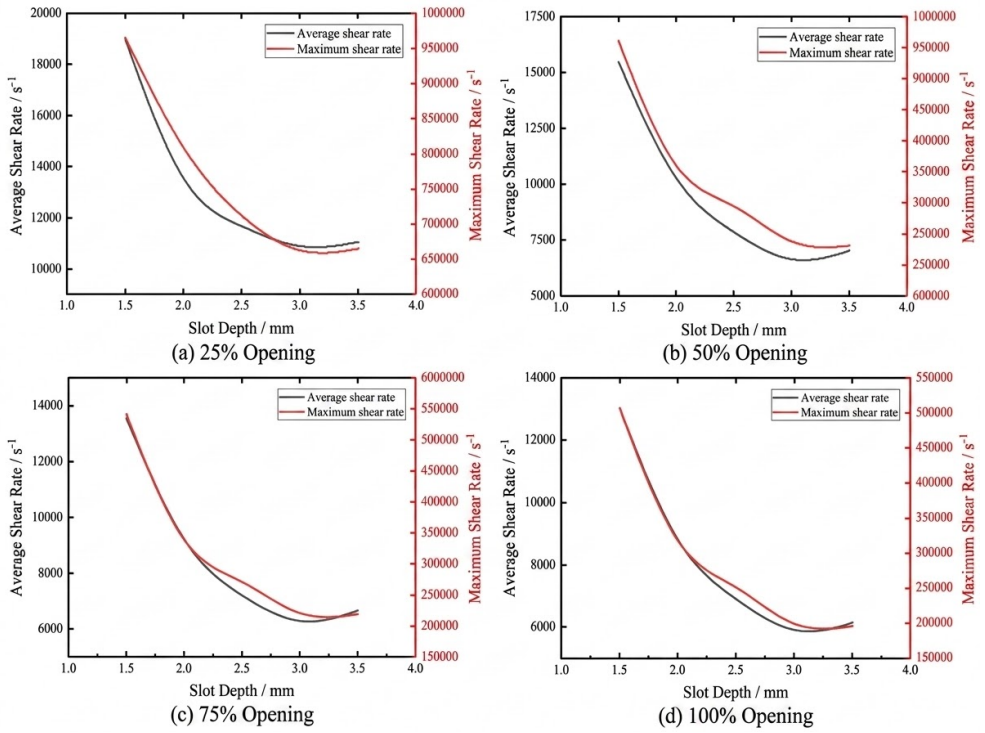

Fig 8. Analysis Result Curve Chart for Different Slot Depths

3.2.3. Influence of Segment Length on Shear Rate

Furthermore, with the groove spacing fixed at 30 mm and the groove depth at 3 mm, numerical simulations were performed to analyze the flow characteristics across various segment lengths (W). The segment length was varied from 1.0 mm to 3.0 mm, with an incremental step of 0.1 mm.

Figure 9 presents the shear rate distribution contours (1) and velocity vector plots (2) for different segment lengths under an inlet flow rate of 5 m^3/h, a valve opening of 50%, a groove spacing of 30 mm, and a groove depth of 3 mm. The results indicate that as the segment length increases, the high-velocity regions within the narrow sections of the flow channel expand, leading to an overall increase in flow velocity. Additionally, it is observed that a longer segment length facilitates the formation of vortex phenomena within the low-velocity zones of the central channel. The internal friction between these vortices and the incoming polymer solution generates significant shearing action. Consequently, a larger segment length results in a higher shear rate within the valve core.

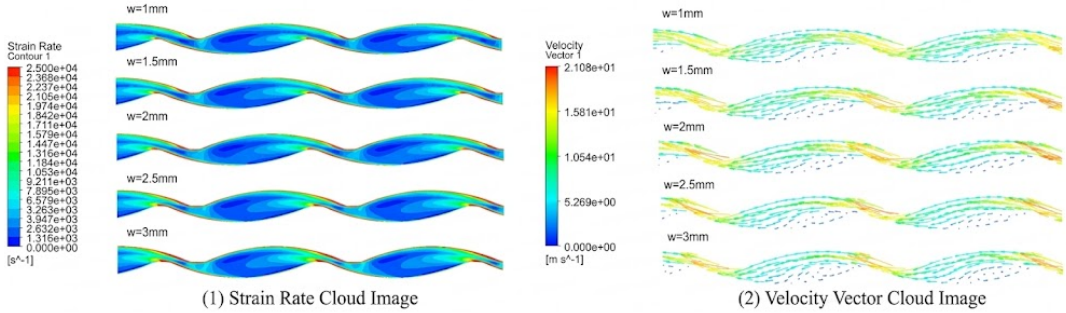

Fig 9. Analysis Contour Plot for Different Valve Stem Lengths

Figure 10 illustrates the comparison of the average and maximum shear rates for different segment lengths across valve openings ranging from 25% to 100%. The curves clearly demonstrate a positive correlation between segment length and shear rate under all four

ISSN: 2688-8645

opening scenarios. As the segment length increases, both the average and maximum shear rates exhibit a consistent upward trend.

The results show that an increase in segment length (1.0–3.0 mm) leads to an elevation in the shear rate. The arc-shaped valve core with a 1 mm segment length achieves the lowest shear rate and demonstrates superior viscosity retention performance. Therefore, 1 mm is identified as the optimal segment length.

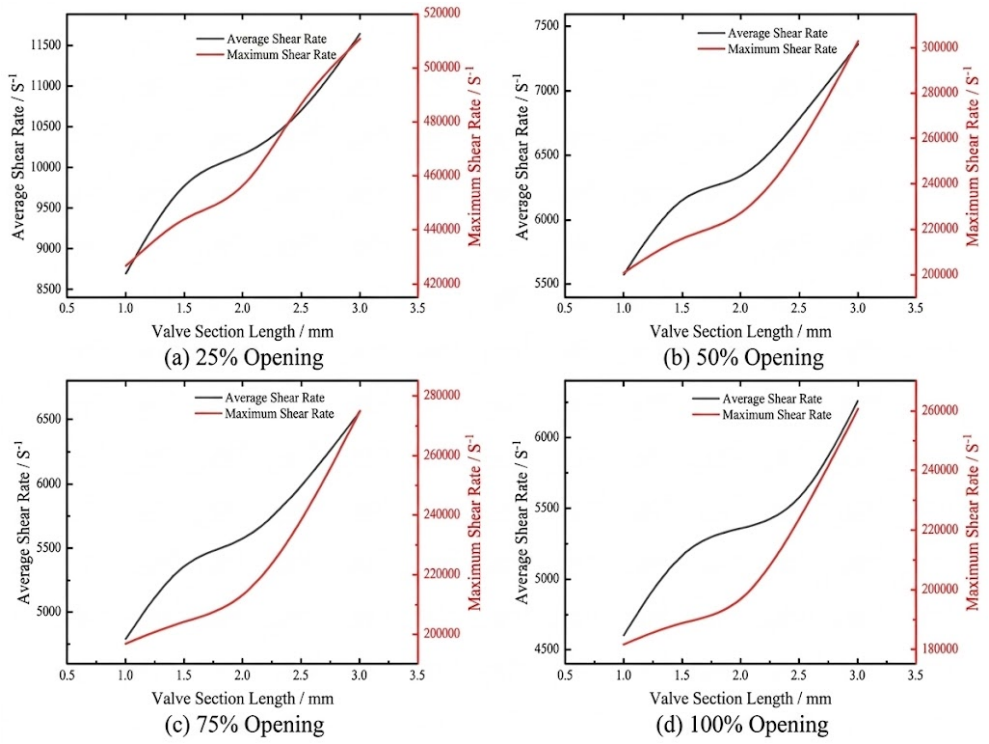

Fig 10. Analysis Result Curve Chart for Different Valve Stem Lengths

In summary, through numerical simulation, the optimal structural parameters for the arc-shaped flow control valve are determined as follows: a groove spacing of 30 mm, a groove depth of 3 mm, and a segment length of 1 mm.

3.3. Structural Parameter Optimization and Validation Based on Orthogonal Analysis

To investigate the influence of the structural parameters of the polymer injection mandrel's valve core on viscosity retention performance, an orthogonal experimental design was conducted based on the previous single-factor optimization. Groove spacing (L), groove depth (H), and segment length (W) were defined as the three independent research factors: A, B, and C, respectively. Three levels were assigned to each factor. The specific factor-level settings are summarized in Table 2.

Table 2. Level Table of Factor 3

Level	Factor A: Groove Spacing L(mm)	Factor B: Groove Depth H(mm)	Factor C: Segment Length W(mm)
1	30	2.0	1.0
2	29	2.5	1.5
3	28	3.0	2.0

ISSN: 2688-8645

Since this experiment involves three factors and three levels, a standard $L_9(3^3)$ orthogonal array was selected, as summarized in Table 3.

Table 3. $L_9(3^3)$ Orthogonal Table

Trial No.	Factor A: L	Factor B: H	Factor C: W
1	1	1	1
2	1	2	3
3	1	3	2
4	2	1	3
5	2	2	2
6	2	3	1
7	3	1	2
8	3	2	1
9	3	3	3

After conducting the experiments, the results were compiled as shown in Table 4. Using the average shear rate as the experimental index, a range analysis (R_j) was performed to determine the significance of each factor's influence on viscosity retention performance. By comparing the mean values ($\overline{K_{ij}}$) of different levels within the same factor, the level with the minimum mean value was identified as the optimal level.

Table 4. Test Results Analysis Table

Trial No.	Factor A: L	Factor B: H	Factor C: W	Experimental Value: X_i
1	A1	B1	C1	9914
2	A1	B2	C3	7667
3	A1	B3	C2	6215
4	A2	B1	C3	10714
5	A2	B2	C2	7728
6	A2	B3	C1	5999
7	A3	B1	C2	10570
8	A3	B2	C1	7521
9	A3	B3	C3	7015
K_{1j}	23796	31198	23434	
K_{2j}	24441	23016	24513	
K_{3j}	25106	19229	25396	
$\overline{K_{1J}}$	7932	7399	7811	
$\overline{K_{2J}}$	8147	7672	8171	
$\overline{K_{3J}}$	8368	6409	8465	
R_j	436	3990	654	

The experimental values X_i in the table represent the average shear rates, where i = (1,2,... 9).

ISSN: 2688-8645

Based on the orthogonal experimental results (Tables 2–4), the calculated range values follow the order $R_2>R_3>R_1$. This indicates that the groove depth (B) has the most significant impact on the shear rate, followed by the segment length (C) and the groove spacing (A). Furthermore, calculations show that $\overline{K_{11}}$, $\overline{K_{23}}$, $\overline{K_{31}}$ are the minimum mean values for factors A, B, and C, respectively. This demonstrates that the optimal parameter combination is A1B3C1 (groove spacing of 30 mm, groove depth of 3 mm, and segment length of 1 mm), which is consistent with the findings from the single-factor analysis.

4. Summary

This study investigated the impact of four common valve core structures on polymer viscosity degradation rates and identified a suitable valve core geometry. Furthermore, by analyzing the influence of various structural parameters of the arc-shaped valve core on the shear rate, the viscosity retention performance of the valve was optimized. The key conclusions are as follows:

(1) Regarding the evaluation of different flow control valve structures, the shear rate of the simulated flow field was employed as the primary indicator of viscosity retention performance. Numerical simulations revealed that, compared to triangular, trapezoidal, and shuttle-shaped configurations, the **arc-shaped valve core** features a smoother flow channel and a wider clearance at the narrowing sections. Consequently, it exhibits a lower shear rate and superior viscosity retention capabilities.

(2) Building upon the arc-shaped valve core design, the study further examined the impact of different structural parameters on viscosity retention. Numerical results demonstrate that the arc-shaped valve core achieves optimal viscosity retention performance with a **groove spacing of 30 mm, a groove depth of 3 mm, and a segment length of 1 mm.**

(3) Experiments and orthogonal analyses were conducted regarding viscosity degradation in the polymer injection mandrel. The **orthogonal experimental results** indicate that **groove depth** is the most significant factor affecting the shear rate. These findings effectively validate the accuracy and reliability of the single-factor simulation analysis.

Acknowledgments

Research on Automatic Vertical Drilling Tool Technology(10351501-19-FW2099-0048).

References

[1] Zhang, L. H., Dong, J. X., Jiang, B., Sun, Y. L., Zhang, F., & Hao, L. (2015). A study of mixing performance of polyacrylamide solutions in a new-type static mixer combination. Chemical Engineering & Processing, 88, 19-28.

[2] Lin, S. (2021). Eccentric zonal injection technology for polymer flooding in L oilfield. Database of Chinese Scientific and Technological Periodicals (Full-text Edition) Natural Sciences, (4), 196-197.

[3] Wang, J. (2015). Research on performance enhancement technology of zonal injection tools for polymer flooding. Oil Production Engineering, (2), 14-17.

[4] Wei, X. F., & Liu, W. (2007). Research and application of mechanical zonal polymer injection technology in Daqing Oilfield. Special Oil & Gas Reservoirs, 14(4), 13-17.

[5] Qian, G. B., Xu, C. F., Chen, Y. K., Wang, X. G., Liu, H. X., & Lian, G. H. (2016). Microscopic mechanism of polymer flooding in conglomerate reservoirs: A case study of the lower sub-formation of Karamay formation in Qidong 1 area, Karamay Oilfield. Xinjiang Petroleum Geology, 37(1), 56-61.

[6] Gao, S., & Bai, M. X. (2018). Numerical simulation of microscopic seepage mechanism of polymer flooding. Journal of Petrochemical Universities, 31(4), 42-45.

[7] Sun, L. D., Wu, X. L., & Zhou, W. F. (2023). Enhanced oil recovery technology by chemical flooding in Daqing Oilfield. Petroleum Exploration and Development, 50(04), 636-645.

ISSN: 2688-8645

[8] Meng, L. Z. (2007). Numerical calculation and application of annular flow field of shuttle-shaped rods [Master's thesis, Daqing Petroleum Institute].

[9] Rojas, M. P., Zanetti, J., Zanetti, S., Stieben, A., & Tidball, E. (2022). Fluid dynamics analysis and performance of polymer flow regulators for polymer flooding in multilayered reservoirs. Journal of Petroleum Science and Engineering, 208, 1595-1599.

[10] Sun, D. X. (2020). Study on viscosity loss mechanism and preparation technology of reservoir polymer flooding injection fluid [Doctoral dissertation, Harbin Institute of Technology].

[11] Ren, Y. L., Sun, K., Lei, Q. M., Gao, S., Xu, Y. J., & Liu, Z. Z. (2018). Viscosity-preserving transformation design of polymer injection pump based on Flow Simulation. Chemical Machinery, 45(3), 387-390.

[12] Han, C. (2017). Numerical simulation and experimental research on a new type of differential pressure injection tool for ASP flooding [Master's thesis, Northeast Petroleum University].

[13] Zhang, H. Q., Zhao, X. M., Wang, Z. H., & Liu, Y. (2020). A method for estimating equivalent shear rate in flow field of crude oil production. Chemistry & Technology of Fuels & Oils, 56(1), 115-123.

[14] Husveg, T., Bilstad, T., Guinée, P. G. A., & Jernsletten, J. (2009). A cyclone-based low shear valve for enhanced oil-water separation. Offshore Technology Conference. DOI: 10.4043/20025-MS.

[15] Zhang, H. R. (2017). Research on key technologies of wireline-retrievable intelligent injection for polymer injection well valve core [Doctoral dissertation, Harbin Institute of Technology].